

We thank the Reviewers for their helpful comments on our manuscript. Below, we present our response to each comment by both Reviewers. The Reviewer comments are given in *italics*, **highlighted with yellow**, followed by our response in plain text. Figures referred to in the responses are shown at the end of this document.

The changes made to the manuscript as per the Reviewer comments are written in **red**.

General changes:

- For a clear presentation of the new ensemble simulations, a new Section 3.3 was created to summarize the model experiment setups.
- Figures 6, 9, 10, 12 and 13 (according to numbering in the revised manuscript) are newly added in response to Reviewer comments. In addition, the figure showing seeding effects on CDNC was switched from vertical profile to a timeseries format (Figure 11 of the revised manuscript).

Reviewer #1

Major comments

There is a lack of a quantitative comparison to results from the observations in J15. ‘..a remarkable resemblance’ (line 227) does not provide enough evidence to support the claim that the ‘model simulations skillfully reproduced the seeding effects. . . as compared with J15’ (line 255). Please can you include values in the manuscript or data in the figures to show this comparison.

The quantitative description of the similarities between the modeled size distributions and those from observations (in J15) will be made more clear and extended. The notion of remarkable resemblance in the original manuscript refers to the increases in concentrations at approximately the 100 μm size range, as well as in droplets larger than about 400 μm . These features are closely associated with similar increases in the observed size distributions, which indicate increased concentrations at around 100-200 μm and above 300-400 μm , sampled near cloud base after the seeding. Moreover, the simulated size distribution shape in general is quite similar to the observations in J15 for the activated droplets (above about 10 μm) with a similar slope as the droplet size approaches 1 mm in the log space.

Additional details and numerical values for comparison are now provided in the text in Section 4.2 lines 280-295 of the revised manuscript.

Other than hydrometeors there is no discussion of the impact to other aspects of the cloud properties. In particular I am surprised that the liquid water content was not presented, as this provides an easy diagnostic to compare to J15 (table 3). There is also no discussion on the radiative impact, nor the temporal evolution of the cloud. For instance, why are there seemingly two peaks in the precipitation rate (Figure 6) at 1 hour and 2 hours? What is the temporal evolution of the CDNC? How long would we expect to see an effect last for? What happens to the sub-cloud fluxes of moisture and buoyancy? What happens to cloud-top entrainment? Do any of these thermodynamic responses counteract or enhance the microphysical effect?

We will add discussion about the cloud temporal evolution in terms of the liquid water content and CDNC. Figures 1 and 2 of this document show the evolution of LWC and CDNC, respectively, near the cloud base in the CTRL and Seed2 experiments. We see that our simulations overestimate the LWC in general (approximately 0.14 g m^{-3} vs 0.09 g m^{-3} in J15 prior to seeding) and that the response to seeding is quite modest, especially if considering the pre and post seeding values in the Seed2 experiment alone, whereas the observed values in J15 show a clear decrease from pre to post

seeding. However, considering the overall low precipitation rate in this case, we remain doubtful, that the seeding effect on precipitation would be enough to yield a considerable decrease in LWC, especially as considerable portion of the precipitation is also evaporated in the below-cloud layer and recirculated back. At the same time, we do recognize that the results suffer from simplifying assumptions, such as the fixed surface fluxes and large-scale subsidence, which are known to affect LWC and thus most likely explain the overestimation, as well as the increasing slope seen in CTRL in Figure 1 of this document.

The CDNC, shown in Figure 2 of this document, generally decreases during the simulation, with somewhat stronger decrease caused by the seeding. The overall decrease is mainly due to the scavenging of CCN by drizzle (we do not include aerosol replenishment in our simulations), collision-coalescence (which allocates droplets to drizzle bins starting from $D=20\text{ }\mu\text{m}$; this limit likely overlaps somewhat with the size range considered as CDNC in the observations) as well as by decreasing vertical velocities, shown in Figure 3 of this document. The runs (the spinup) starts around 4 AM local time and the seeding is started at 8 AM local time, which coincides approximately with the start of the flight legs performed in the field experiment (quoted 16 UTC). Thus, the decreasing vertical velocities and CDNC coincide with reducing cloud top radiative cooling after dawn. As discussed later in this document, the seeding is shown to accelerate the collision-coalescence process, which explains the enhanced decrease in CDNC in Seed2, as compared to CTRL in Figure 2. Again, the change in CDNC between the CTRL and Seed2 experiments is weaker than that attributed to seeding effects in the observations.

The decreasing vertical velocity variability also suggests a general decrease in sub-cloud fluxes during the simulation, but at the same time, the fixed surface fluxes maintain a steady supply of moisture in particular, which we agree is probably not fully realistic.

Further analysis of the radiative effects were left out of the scope of the paper, since the purpose of the manuscript was to show how UCLALES-SALSA represents the short-term seeding effects on precipitation.

The exact explanation for the slightly non-monotonic behavior of the precipitation time series (in Figure 6 of the original manuscript) could not be determined, but is in all likelihood caused by the combination of a small doubly periodic computational domain and random variability associated with the overlapping effects of seeding and the background evolution of the cloud and aerosol. In general, we often see such fluctuations in small-domain simulations and they are typically reduced if the domain size is extended.

Due to the computational cost of the simulations, we did not extend the runs further than approximately 3 hours after the seeding, which is not enough to robustly estimate the longevity of the seeding effect.

The coincident changes in CDNC and in LWC, partly caused by the seeding, surely affect the subsequent cycles of precipitation formation. However, quantifying such feedbacks based on this single case is very difficult because of the very high number of degrees of freedom associated with these variables. Again, the purpose of this work is to show how UCLALES-SALSA compares with the observed microphysical effects in this seeding experiment, as this is the first time the model has been applied for such work. Comprehensive investigation into the sensitivities of the seeding effect warrants a dedicated study covering a wider range of conditions.

LWC and CDNC are now shown in Figures 10 and 11 and discussed in Section 4.1 lines 239-250 in the revised manuscript.

The discussion section needs to be expanded. There is no discussion on uncertainties that may arise due to the model microphysics. Are there any? As the authors point out the results may be impacted due to variations in the meteorology – there are many studies focusing on MSCs that could be used to provide examples of how the results may be affected. For example, the cloud dynamics are highly sensitive to the buoyancy profile – too strong surface fluxes or cloud-top entrainment rate may make your cloud more or less susceptible to changes in CDNC. Could this be a possible reason you don't see the same 'seeding efficacy' as J15? I believe the authors should spend more time discussing this. Finally, have there been any other cloud-seeding modelling studies? How do the conclusions and results compare? Can this study be compared with other MSC modelling studies focusing on aerosol-cloud-interactions?

We will extend the discussion on the model uncertainties, which surely do arise both from the numerical representation of processes as well as from the initial conditions. Following the suggestions by Reviewer #2, we have performed a series of sensitivity tests, which show that the results are somewhat sensitive to e.g. the boundary layer moisture content. Moreover, simplifying assumptions like the fixed surface fluxes and large-scale subsidence most likely reduce the realism of the simulations, as discussed above. We will extend the discussion as suggested.

Modeling studies on cloud seeding exist, some of which have already been referenced in the manuscript. We will enhance the discussion of our findings with further references. Regarding studies on aerosol-cloud interactions, the works by Jensen et al. for example on the role of GCCN in precipitation formation are of course very relevant to this work and have already been cited in the manuscript. We will reiterate these in the discussion. Considering studies on aerosol-cloud interactions in MSC in a more general context, we should investigate more carefully the impact of cloud adjustments over a longer period of time and changes due to a broader spectrum of particle sizes, which goes outside the scope of the current paper.

Discussion about uncertainties in the simulations is added on lines 359-377 of the revised manuscript, including extended discussion about the reasons for the weaker than observed seeding effects. Some discussion about the results of the current manuscript to other studies is added also in lines 330-333 and 343-346.

Minor comments:

Title. I believe airbourne should be spelled airborne.

The spelling is corrected in the revised manuscript

Correncted throughout the text.

Line 63 (Model description): how is mixing of air parcels represented? e.g., homogeneous or inhomogeneous?

The subgrid scale mixing is homogeneous.

Line 118: The 8.5K inversion strength appears a lot stronger than in J15. Is this correct? What impact does this have on the simulations?

The upper boundary of the inversion layer is not particularly well defined in the measured profiles (J15 figure 3), so our interpretation was to set the inversion layer in the model as the layer between approximately 650 and 700 m, between which the observed potential temperature changes from about 288 K to 296.5 K or so, resulting in 8.5 K, which is quite typical for marine Sc. One could argue that the observed inversion layer stops at around 293-294 K, which would yield about 5-6 K inversion strength. However, the observed potential temperature slope above this level continues as approximately 5 K/100 m, which is still much more stable than one would generally expect for the lower troposphere above the boundary layer.

Line 120: Why were fluxes and subsidence prescribed according to Ackermann 2009?
Were values for the campaign not available? Are they appropriate for the time and place of the campaign? Please include these values in the manuscript. Also, I presume being prescribed they are not interactive. Please clarify this in the text.

We are not aware of these values specifically from the observed period reported in J15. However, the field experiments took place approximately in the same area and the same time of the year as DYCOMS-II, for which the values in Ackermann (2009) are accepted as a general reference, so most likely they are representative of the local conditions. These values are indeed fixed and not interactive, which simplifies the setup, but does reduce the realism of the simulations, as discussed above. We will make the suggested additions to the revised manuscript.

The values are given on lines 119-122, where we also note they are prescribed.

Line 113 (Initial conditions): Was there any vertical damping applied within the domain?
Please clarify in text.

A damping layer is present in the top 100 m of the model domain throughout the simulation. We will mention this in the manuscript.

Added to line 124 of the revised manuscript.

Line 140: What is the objective of using a domain-wide injection? This isn't realistic so there must be a reason for it?

The objective was to map the effect of different emission strategies, including the extreme (yet surely not practical) case of domain wide injection. Essentially, this affects the total emitted mass and the mixing dilution of the seeding aerosol. We will clarify this in the manuscript.

Added explanation to lines 145-146 of the revised manuscript.

Line 143: vertical cross-section?

Corrected.

Line 162: What are the total masses released for each of the three experiments and how does this compare with the campaign?

Calculated simplistically from the mode mean diameters, in Seed1 the mass released is approximately 20 kg and in Seed2 it is 200 kg. In the domain wide seeding setup (Seed3) the released mass is approximately 4000 kg. Obviously, Seed3 does not portray a realistic scenario and was performed exclusively to investigate the sensitivity of the simulated seeding effect. It shows that in terms of the total released mass, the seeding effect shows signs of saturation, although we don't expect to be able to robustly estimate this saturation point using a periodic boundary conditions for the model domain.

We note that the released mass in the simulations depends strongly on the assumption about the volume occupied by the initial plume (the assumed plume cross-section was 50 x 50 m²). J15 do not directly quote the total mass they released in the field experiments. Therefore, we instead targeted the plume concentrations after allowing some time for mixing, which J15 estimated to be at maximum on the order of 10⁻² cm⁻³, which we also reached in our simulations (Figure 7).

Figure 7 → Figure 8 in the revised manuscript.

Line 167: What is the simulated precipitation rate that is ‘rather low’?

Line 167: J15 table 3 states a pre-seeding precipitation rate at the cloud base of 0.04 mm/hr - why was 0.05 used to constrain the control case?

As a response to the two comments above: The statements on the precipitation rate were directed to the case in general, since the overall precipitation rates, both in model and observations, are indeed quite low. We will reword this sentence in the revised manuscript to make it more clear. The mentioned observed precipitation rate should indeed be 0.04 mm hr^{-1} , which will be corrected. But we did not use this information to “constrain” the simulated precipitation rates.

Made the reference to observed values (and corrected the values) more clear in lines 181-182 of the revised manuscript.

Line 168: On seeding efficacy.. this sounds like this should be a metric for dP/dM and is something I was expecting to be quantitatively evaluated later in the manuscript. Is this possible? It could provide a good way to compare different models or observations. . .

Perhaps this is a misuse of terminology on our part. We simply refer to the magnitude of the seeding response or seeding effect. We will revise the use of this terminology in the manuscript.

The terminology is changed away from “efficacy” throughout the manuscript as stated in the response.

Line 184: It is stated that ‘10m vertical resolution has been shown to be inadequate to fully represent the effects of entrainment mixing’ yet the 10m vertical resolution is used. Is entrainment not an important process? Did you see differences in entrainment rate between the two simulations? Were there any changes to other BL processes?

Here we are mainly concerned with the sensitivity of precipitation to the resolution. It is true, that works such as Stevens et al. (2005) point out the challenges of representing entrainment mixing even with resolutions much higher than 10 m. However, this comes with a significant increase in the computational cost, which is already very high in our model. In spite of this, the sensitivity tests already reported in the manuscript showed a convergence of results in terms of the precipitation rates at 10 m resolution, so this was selected for our main experiments as a compromise between accuracy and computational cost. Nevertheless, we do not claim that this would provide a perfect representation of the entrainment mixing.

Line 189: What is the cloud base height?

About 250 m after the seeding.

Mentioned in Section 4.1 line 210.

Line 195: What is the injected mass?

Please see the response for Line 162.

Line 199: Can you provide an estimate of how quickly the particles are activated?

Since the particles are in the micrometer size range, injected into saturated cloudy air, within a few timesteps.

Line 204: Can you please provide a value for how long ‘not long’ is?

The timescale is about 10-15 minutes, we will reiterate this in the manuscript.

Added on line 224 of the revised manuscript.

Line 206: Could you provide a description for seeding efficacy?

As stated above, we simply refer to the magnitude of the seeding response or seeding effect. We will revise the use of this terminology in the manuscript.

The terminology is changed away from “efficacy” throughout the manuscript as stated in the response.

Line 207: Please change ‘concentration’ to ‘concentration of seeding particles’.

Done.

Correction found on line 228.

Line 208: Is this simply the mean of the Seed2 profile in figure 7? Please could you clarify in the text.

Added “... suggested by the mean of the Seed2 profile in Figure 7”

It now says “The mean of the Seed2 profile in Figure 8 suggests that in order to produce an approximately 2-fold precipitation yield, the concentration of seeding particles mixed in the cloud layer should be on the order of 0.01 cm^{-3} ” on lines 227-228 of the revised manuscript.

Line 210: is this statement just for MSCs or for all cloud types?

In a more general context, yes these pathways are hypothesized also in convective clouds in the case of hygroscopic cloud seeding, even though in convective clouds the dynamical perturbations and mixed-phase processes become relevant and make the issue more complex. Therefore, in line with the focus of this manuscript, we will mention the focus on warm clouds in this sentence in the revised manuscript.

The focus on warm low-level clouds is mentioned on line 252.

Line 214: A crux of the argument for dismissing water-vapour competition (between ambient and seeded particles) is based on the RH yet this is not shown, nor are values provided. Please include this. Also, do other modelling studies see the same response? For example, MSC modelling studies with above-cloud plumes (such as in the SE Atlantic) are potentially analogous to this seeding experiment..

We will include a figure showing the supersaturation profile averaged over updraft areas, where only very minor decrease is seen around cloud base for Seed2 and Seed3 (shown in Figure 4 of this document). In addition, as per request by Reviewer #2, we have also analyzed the effect of seeding to the process rates using the new set of sensitivity tests. The results do not indicate any significant effect in the cloud activation rate caused by the seeding. However, a significant effect is seen in the mean drizzle formation rate, which we derive directly from the collision-coalescence process in our model.

The new Figure 12 shows the in-cloud supersaturation and the new Figure 13 shows the microphysical process rates. Corresponding discussion is added on lines 257-277 of the revised manuscript.

Line 217: The competition between activation of ambient and seeding particles is discussed, but what about competition between ambient droplet growth and activation of seeding particles at cloud top? Does this enhance or suppress the width of the DSD?

The competition for water vapor surely does have an effect on the growth of droplets. Since UCLALES-SALSA solves condensation equations for water vapor in non-equilibrium conditions in

a size-resolved framework, the model does allow the injection of particles larger than the background population to shift the allocation of water from smaller to larger CCN, whose equilibrium saturation ratio is smaller. This would contribute to the increase DSD width. However, this effect depends on the particle concentration and is not easily distinguished with the relatively small concentration of the seeding aerosol. This discussion will be added in the manuscript.

We have added this consideration on lines 339-343 of the revised manuscript.

Line 219 / Figure 8: Why does the cloud base and cloud top height change with increasing seeding mass?

The figure is a bit misleading, because we zoom the x-axis into larger values in CDNC in order to show the difference between the experiments more clearly. We don't see a clear change in the cloud boundaries due to seeding, at least in the relatively short timescales investigated. We will make this clear in the caption.

We ended up replacing this figure with a timeseries of CDNC, which was requested by the Reviewer. The original was removed in favor of avoiding overlapping information and limiting the number of figures. In the revised manuscript, the CDNC is shown in Figure 11.

Line 219: How much of the decrease in CDNC is attributed to increased removal via precipitation?

We attribute the change in CDNC between the control and seeding experiments to be primarily due to collision-coalescence and accretion by drizzle and rain drops as noted above. However, we cannot robustly quantify the direct contribution of precipitation fall-out to CDNC decrease in particular, since we can not track the number of collisions undergone by each drop.

Extended discussion about CDNC is added in lines 360-364.

Line 224 to 230: Referring back to a previous comment please make this comparison to DSDs in J15 quantitative, including the terminology (e.g., ‘..bear a remarkable resemblance to..’). Including the DSDs from J15 onto the figure 9 would provide a very good comparison.

We will provide a more quantitative description.

A revised discussion on this is found on lines 278-295 of the revised manuscript.

Line 234: Saying 5 hours is confusing – change to 1 hour after emission or something to that effect..

We will follow the suggestion.

It now says “1-1.5 hours after the seeding emission” on line 299 of the revised manuscript.

Line 249: ‘In successful cases’ do you not see this in all three cases?

Yes we do, we will remove this from the manuscript.

Removed

Line 249: ‘sustained effect up to 2-3 hours’ without extending the simulation length you can’t really give a maximum timescale. Please clarify.

This is true, as we also mentioned in a comment above. We will revise this statement accordingly, that we cannot robustly estimate the longevity of the effect using the data we have.

It now says “... sustained effect lasting until the end of the simulations” on line 322.

Line 250: ‘peak enhancement. . . within 1-1.5 hours’ Seed1 and Seed2 appear to reach a maximum enhancement at \sim 2hours. Please clarify.

This statement will be revised as suggested.

This is corrected on line 323 of the revised manuscript.

Line 253: ‘on the high end of the diluted plume concentration. . . i don’t think this was ever discussed before - what were the estimated concentrations in J15?’

J15 estimated the plume concentrations to be in the range from 10^{-2} ... 10^{-4} cm⁻³. We will note this in the revised manuscript.

Added on lines 326 of the revised manuscript.

Line 255: ‘The model simulations skillfully reproduced..’ What measure of skill was used? Perhaps replace skilfully with qualitatively unless the quantitative comparison is provided in section 4.2.

We will revise this statement accordingly.

It now says “...the model simulations reproduced the main features of the observed seeding effects on the hydrometeor size distribution...” on lines 347-348 of the revised manuscript.

Line 268: Are there other processes that could produce the required concentration?

Unfortunately, we are unsure what this question refers to?

Discussion section: Are the results and conclusions applicable to different locations? MSCs have a very strong diurnal cycle – what would happen if the seeding took place at a different time when the MSC may be more sensitive to the perturbation?

In the pilot runs performed when preparing the model experiments we saw that the results are somewhat sensitive to the droplet concentration, and the results in the mini ensemble introduced in our response to Reviewer #2 show that the results are also sensitive to the boundary layer moisture content. Also, according to J15, Aug 3 case was the only one where significant seeding effects were measured from the number of flights conducted during the field campaign.

Therefore, we do expect the seeding effects to change diurnally as well as in different regions. The result are also somewhat sensitive to the model initial conditions. We feel that a more in-depth study into the different sensitivities goes beyond the focus of the current manuscript and should be investigated in a separate paper. The purpose of the current work is rather to present the ability of UCLALES-SALSA to represent the basic microphysical processes controlling the seeding effect, than to provide a comprehensive estimate of the sensitivities of the rain enhancement.

Discussion on this is added on lines 367-371 of the revised manuscript.

Throughout figures: ‘function of time’ please clarify what time this refers to - since injection I presume?

This is correct, we will clarify this in the manuscript.

Noted that the time is relative to seeding injection time in all the relevant figure captions.

Figures 7,8,9,10. The manuscript refers to concentrations in units of cm-3 and diameters in um - but these figures are in m-3 and m. Please update figure axes units so that

they are consistent with the usage in the manuscript.

We will make this correction.

The units in figures and text are now consistent.

Reviewer #2

1. Uncertainties associated with the simulations

It is probably well known that the evolution of a nonlinear system such as the atmosphere is very chaotic and sensitive to initial conditions and any perturbations. For a numerical model that simulates the atmosphere dynamics and relevant physics in an Eulerian framework, errors from the numeric are inevitable to propagate across the domain when sensitivity experiments are conducted (Ancell et al. 2018). It is reasonable and probably recommended to conduct ensemble simulations of the control and sensitivity experiments using perturbations in initial conditions (such random noise in thermodynamics and the back ground aerosol concentration) and some physics parameters (such as the large-scale subsidence rate) to separate the physical responses of the sensitivity experiment from the natural and numerical uncertainties. Or, the authors can apply the “piggybacking” methodology proposed by Wojciech Grabowski (Grabowski 2014; 2015 and many others) to single out the microphysical impacts in this case. Though the authors mentioned the multi-realization approach of this study, I did not see the spirit of the ensemble approach in this case.

We do appreciate the sensitivity of the simulations to perturbations in initial conditions and to numerical uncertainties. However, we do think the solid steady stratocumulus deck, such as in our simulations, is a relatively straightforward environment to test specific microphysical effects, like the cloud seeding.

Unfortunately, running large ensembles covering extensive parameter space is not practical with our model because of its very high computational cost. Moreover, we have considered implementing the piggybacking methodology in our model, but complexities arising from the full bin treatment of the microphysics have so far refrained us from engaging in this action, and therefore it is not pursued in the scope of this revision.

Nevertheless, we have performed a small ensemble with 20 members, each assigned with a randomly selected pair of values for the initial boundary layer moisture content and the large scale subsidence so that the samples are within $\pm 10\%$ of the ones in the original manuscript. Figure 5 of this document shows the rain enhancement due to seeding as a scatter plot, where we see that varying the subsidence (within the 10 % range) has a minor effect on the precipitation enhancement by seeding, while varying the boundary layer moisture has a more pronounced effect. However, in terms of the relative change in precipitation, the results are more uniform and suggest a stronger relative change for lower moisture content (and lower overall precipitation), which is somewhat expected.

The additional sensitivity experiments provided here as well as the data already present in the manuscript do show, that the results are sensitive first of all to the specifics of the seeding operation and also to the initial and boundary conditions of the model. In addition, the bin representation of the particle size distributions comes with inherent uncertainties related e.g. to numerical diffusion as well as to the process representation, as do any other microphysics schemes. However, based on all of our data, the cloud seeding effect in this case remains qualitatively consistent. We also note, that the case on 3 Aug was the only case in the field experiment where J15 reported a significant observed seeding effect. The purpose of the current work is to show the ability of UCLALES-

SALSA to represent the seeding effect in this case, instead of pursuing an exact case study or estimating the full range of sensitivity of the seeding effect to various factors. The simulated seeding effects on the microphysics, particularly the droplet size distributions, are in agreement with the observations and, together with the rather consistent rain enhancement seen in our data, this is an encouraging result.

The description of the ensemble simulation setup is given in the last paragraph of Section 3.3 of the revised manuscript. There was a slight error in the precip enhancement scatter plot image of the author response submitted earlier which caused the values to be a bit too low. Fixed image is now included in the manuscript (Figure 9). The ensemble results are discussed in Section 4.1 on lines 229-238 and Section 4.2, lines 258-275.

2. Hypothesis test

I understand that the purpose of this study is not to test any of the hygroscopic seeding hypotheses as mentioned in the introduction. But when I saw the authors speculating the hypothesis of increasing C-C by introducing GCCN as rain embryos from the cloud top led to the reduced CDC as discussed in Fig. 8, I could not help suggesting the authors to spend slightly more effort to prove or disprove this point. Could it be possible that these GCCN are mixed through the cloud volume by turbulence and start to suppress background aerosol activation at cloud base (Fig 7 kind of show this in action)? The authors should be able to configure the model and test out these hypotheses, which will contribute to the field more significantly than the current form.

Using the results from the mini ensemble, we included additional diagnostics for process rates. Indeed, the autoconversion rate, derived directly from the collision-coalescence process (sampling the rate of collisions producing drizzle) within the model, shows a clear peak after the seeding in Figure 6 of this document. However, the cloud activation rate shown in Figure 7 of this document does not show a clear signal in either direction, other than the gradual decrease caused by the radiatively induced decrease in vertical velocities and the gradual scavenging of CCN. In addition, as requested by Reviewer #1, we will include a figure showing the supersaturation profile averaged over updraft areas (Figure 4 of this document): this shows that in Seed2 and Seed3 the supersaturation is decreased, but the magnitude of the change is very small, and not enough to yield significant changes in the activation rate.

We will elaborate on the GCCN effect in the manuscript using the process rate diagnostics.

The process attribution is discussed in Section 4.2, lines 258-275 and the rates are analyzed in Figure 13 of the revised manuscript.

3. Model setup and analysis

The authors show the sensitivity of the simulated precipitation flux to the vertical resolution. How sensitive are the results to the prescribed large-scale subsidence? According to Chen et al. (2010), the simulated clouds are sensitivity to this factor.

In the context of the mini ensemble, the seeding results are not particularly sensitive to small variations of the subsidence rate. However, our simulations do show sensitivity to larger changes in subsidence, such as those presented in Chen et al. (2010). For this, we rerun the control simulation with the large-scale divergence set at 8.0e-6. This causes the precipitation rate to decrease significantly, to about 0.01 mm h^{-1} , as shown in Figure 8 of this document. This result is qualitatively in agreement with Chen et al. (2010), even though not directly comparable because of the shortness of our simulations and the simplified treatment of the diurnal cycle.

The sensitivity to subsidence is discussed in the last paragraph of Section 3.4 and shown in Figure 6 of the revised manuscript.

How long did you simulate the seeding operation? That basically gives you the total seeding particles released in your model domain. By assuming a well-mixed MSc boundary layer, you can easily calculate the seeding particle concentrations from each experiment.

In Seed3 all the particles were released during a single timestep. In Seed1 and Seed2 the release along the trajectory with the assumed airspeed of the source at 60 m s^{-1} takes about 8-9 minutes. The estimated concentration of the seeding particle plume slightly after release is shown in Figure 7. The particle release rates are commented on in Section 3.2. Please also refer to our response to the comment about Line 162 by Reviewer #1.

In the revised manuscript, these are now Section 3.3. and Figure 8.

How do you treat the sedimentation of the GCCN particles?

In practice this undergoes a similar treatment as cloud droplets. With SALSA we know the wet diameter of the particles/droplets. With that we calculate the terminal velocity according to a simple set of equations found in R.R. Rogers: A Short Course in Cloud Physics,(Pergamon Press Ltd., 1979) and calculate the flux divergence to determine the change in particle concentrations in consecutive levels, taking also into account the associated effects on latent heat.

In order to support the hypothesis associated with the Fig. 8, the authors should directly compare the microphysical process rates (C-C rate) from the model outputs. As what the study shows right now, we don't know what happens exactly.

Please see our response in the previous section.

This is now shown in Figure 13 and discussed in Section 4.2 lines 258-275 in the revised manuscript.

The topic of this manuscript is on rain enhancement. Would it be more helpful to show the effects from seeding on ground precipitation amount and distribution?

The purpose of this work was to demonstrate how UCLALES-SALSA represents the seeding effects in the case based on field observations. The measurements in the field experiment were performed using an airborne platform at the height of cloud base as well as in-cloud, so we wanted to perform the analysis with similar sampling strategy. However, qualitatively similar increase in precipitation is seen close to the surface as well, albeit smaller in magnitude due to evaporation.

Technical issues:

Line 20: I will replace “somewhat” with “very”.

Done.

Line 21: “true effects” is not an appropriate expression.

Removed “true”.

Line 158: shown in Figure 3.

Corrected.

Precipitation enhancement in stratocumulus clouds through ~~airborne~~ airborne seeding: sensitivity analysis by UCLALES-SALSA

Juha Tonttila¹, Ali Afzalifar³, Harri Kokkola¹, Tomi Raatikainen², Hannele Korhonen², and Sami Romakkaniemi¹

¹Finnish Meteorological Institute, P.O. Box 1627, 70211, Kuopio, Finland

²Finnish Meteorological Institute, P.O. Box 503, 00101, Helsinki, Finland

³Aalto University School of Science, Department of Applied Physics, Espoo, Finland

Correspondence: Juha Tonttila (juha.tonttila@fmi.fi)

Abstract. Artificial enhancement of precipitation via hygroscopic cloud seeding is investigated with a numerical large-eddy simulation model coupled with a spectral aerosol-cloud microphysics module. We focus our investigation on marine stratocumulus clouds and evaluate our model results by comparing them with recently published results from field observations. Creating multiple realizations of a single cloud event with the model provides a robust method to detect and attribute the seeding effects, which reinforces the analysis based on experimental data. Owing to the detailed representation of aerosol-cloud interactions, our model successfully reproduces the microphysical signatures attributed to the seeding, that were also seen in the observations. Moreover, the model simulations show up to a 2-3 fold increase in the precipitation flux due to the seeding, depending on the seeding rate and injection strategy. However, our simulations suggest that a relatively high seeding particle emission rate is needed for a substantial increase in the precipitation yield, as compared with the estimated seeding concentrations from the field campaign. In practical applications, the seeding aerosol is often produced by flare burning. It is speculated, that the required amount of large seeding particles suggested by our results could pose a technical challenge to the flare-based approach.

1 Introduction

Water scarcity is a cause for increasing concern in arid as well as in semi-arid regions (WWAP, 2019). This has revived the interest in research and investments in weather modification efforts, particularly those related to ~~rain~~ precipitation enhancement (Flossmann et al., 2019). One of the prominent methods is to purposely introduce large hygroscopic particles into a cloud, which act as cloud condensation nuclei (CCN) and are expected to enhance the growth of droplets and therefore the production of drizzle and precipitation (Bruintjes, 1999; Kuba and Murakami, 2010; Rosenfeld et al., 2010). In spite of numerous experiments on hygroscopic cloud seeding (e.g. Cotton, 1982; Bigg, 1997; Ghate et al., 2007; Jung et al., 2015), estimates of its effect on rainfall are still ~~somewhat~~ very uncertain. Given the present consumption rate, the problem of water shortage will most likely

become worse, urging for more systematic research efforts to improve the scientific basis for understanding the ~~true~~-effects of seeding with hygroscopic particles.

Attribution of observed effects to artificial perturbations is an intrinsic issue in most field experiments investigating weather modification methods, which makes it difficult to reach a consensus about their applicability. In the case of ~~rain~~precipitation enhancement, it is often problematic to detect the precipitation response to seeding and, in particular, to distinguish it from meteorological variations (Flossmann et al., 2019). Field experiments only provide a single realization of an event: as soon as the cloud is seeded, the reference point is lost, causing it to be very difficult to estimate the unperturbed precipitation rate. This challenges the reproducibility of results from cloud seeding field experiments. Instead, modelling studies provide the advantage of generating multiple realizations of each scenario and, with a carefully planned setup, the experiments are reproducible. Cloud-resolving models comprise an important source of information to complement field campaign studies, as they provide a highly controlled environment for repeatable experiments ~~on the seeding efficacy~~to estimate the seeding effects, which helps to tackle the attribution issue. In this paper, we employ a cloud resolving large-eddy model with sophisticated representation of aerosol-cloud microphysics to study the effects of seeding in marine stratocumulus clouds, which arguably provide the simplest environment where to untangle the governing microphysical processes.

The way in which hygroscopic cloud seeding is expected to influence precipitation is closely related to the effects of naturally occurring giant CCN (GCCN; diameter larger than $1\text{ }\mu\text{m}$) and can therefore be considered as being part of the ongoing efforts to understand the aerosol-cloud interactions. In marine boundary layers, GCCN consisting of sea salt is a prominent feature (Jensen and Lee, 2008; Bian et al., 2019). Due to their initial size and the large amount of soluble material, GCCN grow relatively fast in saturated conditions by water condensation and may continue to grow even in a slightly ~~subsaturated~~sub-saturated environment (Jensen and Nugent, 2017). The presence of GCCN in a cloudy boundary layer has been noted for increasing the mean droplet size and producing higher amounts of precipitation both in experimental (e.g. Lehahn et al., 2011; Dadashazar et al., 2017) and modelling studies (Feingold et al., 1999; Jensen and Lee, 2008; Jensen and Nugent, 2017). The effect of GCCN is caused by two different microphysical mechanisms. First, they suppress the maximum supersaturation during droplet formation due to their water uptake, and thus decrease the total number of cloud droplets. This will yield on average larger droplets and potentially faster precipitation formation. Second, hydrated GCCN increase the width of the cloud droplet size distribution and are thus expected to enhance the collision-coalescence process leading to an increase in precipitation. Additionally, very large wetted GCCN particles may directly contribute to precipitation by acting as raindrop embryos. These processes lay the basic foundation for the hypothesis of hygroscopic cloud seeding to enhance rainfall as well (Kuba and Murakami, 2010; Rosenfeld et al., 2010). The seeding particles, most often delivered to the cloud layer via an aircraft, are typically released by burning flares or from containers with ~~premanufactured~~pre-manufactured milled salt powder (e.g. Jung et al., 2015). It is generally agreed, that the seeding particles need to be in the size range of several micrometers in order to be effective in warm clouds (Segal et al., 2004; Rosenfeld et al., 2010).

In the current work we explore the sensitivity of drizzle and precipitation in marine stratocumulus to hygroscopic cloud seeding using the UCLALES-SALSA (Tonttila et al., 2017) large-eddy model. This modelling package combines the UCLA Large-Eddy Simulation code (UCLALES; Stevens et al., 2005) with the highly detailed microphysical representation by the

Sectional Aerosol module for Large-Scale Applications (SALSA; Kokkola et al., 2008). We will investigate the seeding effects in a marine stratocumulus setting based on measurements from a recent field campaign study (Jung et al., 2015). The results serve the purpose of evaluating the ~~skillability~~ of our modelling platform ~~in reproducing to reproduce~~ the observed microphysical effects as well as to map the importance of the seeding injection strategy and emission rate in terms of the precipitation 60 yield. The remainder of this article continues with the description of the current version of the UCLALES-SALSA model in Section 2. The experimental setup for the model and the specific settings applied in the simulations are summarized in Section 3 followed by description of the results in Section 4. Conclusions are drawn together with some further discussion in Section 5.

2 Model description

65 UCLALES-SALSA (Tonttila et al., 2017) is built around the well established UCLALES (Stevens et al., 2005) large eddy simulation code, which comprises a modelling platform for idealized cloud simulations. The model uses a 3-dimensional computational mesh with cyclic lateral boundary conditions, including a prognostic description of the three Cartesian wind components. The advection of momentum is based on fourth-order difference equations with time stepping scheme based on the leapfrog method. The prognostic scalar variables include the liquid water potential temperature and variables describing 70 water vapor and condensate amounts, depending on the model configuration. The scalar advection uses a second order flux-limited scheme and the time integration is performed with a simple Eulerian forward time stepping method.

The aerosol and cloud microphysics are represented by the SALSA module. The design of SALSA is described in detail in Kokkola et al. (2008) and Tonttila et al. (2017), but key features are also summarized below, including a description of some 75 important updates. The general layout of the current SALSA module is illustrated in Figure 4.1. SALSA is a bin microphysics model, describing the size distribution and composition of particles in up to four different categories: aerosol particles, two sets of liquid hydrometeors (cloud droplets and a separate regime dedicated for droplets and precipitation dominated by collision-coalescence growth) and ice (not used in the current work and thus not shown in Figure 4.1). For aerosol particles and cloud droplets it is possible to use two parallel sets of bins in order to describe externally mixed aerosol populations with separate size distributions.

80 For particle composition (in all categories), the model uses up to five different aerosol constituents (sulfate, sea salt, organic carbon, black carbon, dust) plus water. Each parameter (particle number and mass of each constituent) in each bin comprises a prognostic scalar variable in UCLALES-SALSA. The model solves all the key microphysical processes for all particle categories, including cloud activation, coagulation and collection processes as well as the condensation of water vapor on both aerosol particles and hydrometeors (see Tonttila et al. (2017) for further details).

85 The design of SALSA is an attempt 1) to find a compromise between computational cost and model accuracy and, in particular, 2) to be able to track both ~~the~~ non-activated and activated particle populations. The latter ~~in particular~~ is fulfilled by setting both the aerosol and cloud droplet bin limits according to the dry aerosol or CCN particle diameter, as illustrated in Figure 4.1. This allows to preserve the characteristics of the aerosol size distribution at the aerosol – cloud droplet interface.

As seen in past model experiments (Tonttila et al., 2017; Boutle et al., 2018), it also provides an adequate description of the droplet size in order to solve the in-cloud microphysical processes. The ability to track the aerosol size distribution in and outside of clouds brings the model a step further from more straight-forward 1-d bin model designs, where information about activated aerosol is not explicitly tracked. This is also a very important feature for this study, since tracking the evolution of the seeding particles within the cloud is key in order to capture their influence on cloud microphysics and rain formation as well as to analyze and understand the underlying processes.

An important upgrade not described in previous papers concerns the description of precipitation. In the current version, the size distribution for drizzle and rain is described by 20 mass doubling bins (in the wet diameter space) starting from $20\text{ }\mu\text{m}$. Moreover, instead of a parameterized autoconversion process, we now determine the transition from cloud droplet to drizzle regime directly from the coagulation code. If the droplet diameter resulting from the collision-coalescence between two cloud droplets exceeds the $20\text{ }\mu\text{m}$ limit, the outcome is moved to a drizzle bin with appropriate diameter range. Obviously, the $20\text{ }\mu\text{m}$ limit separating cloud droplets and drizzle is quite small. The decision for this limit was made in favor of more accurate resolution of the droplet size in wet diameter space, where the droplet growth begins to be dominated by collision-coalescence. This helps to ensure a smooth transition from cloud droplets through intermediate sized drizzle (Glienke et al., 2017) to full size drizzle drops and eventually rain. It also provides a more accurate method to describe the growth and transport of GCCN particles within the diameter space, than what was possible with the previously used parameterized autoconversion method (Tonttila et al., 2017).

3 Model setup

Marine stratocumulus clouds have been used as the setting for numerous field experiments looking into aerosol-cloud interactions. In a recent study (Jung et al., 2015, henceforward J15), rain precipitation enhancement by hygroscopic cloud seeding was investigated from airbourne airborne observations, that took place southwest of Monterey, California, on 3rd August, 2011. We will use this case as the basis for the model experiments in this paper. The meteorological data and aerosol characteristics presented in J15 are used to provide the initial conditions for UCLALES-SALSA. We exploit this setup to investigate the ability of UCLALES-SALSA to simulate the cloud microphysical response to hygroscopic seeding in a series of experiments, consisting of a control run and three cloud seeding runs with different seeding strategies, whose details are outlined below.

3.1 Initial conditions

The measurements reported in J15 took place starting from 16 UTC. We match the model time with this period, which mainly affects the radiative budget at cloud top via the solar zenith angle. The initial profiles of potential temperature and the total water mixing ratio are shown in Figure 22, where the moisture profile is saturated between the levels of approximately 300 m and 650 m. The strength of the potential temperature inversion at the top of the cloud (after condensation of the excess moisture from Figure 22) is approximately 8.5 K. For simplicity, the horizontal wind is initialized to $u = -12\text{ m s}^{-1}$, $v = 0\text{ m s}^{-1}$, following the standard meteorological notation, which corresponds to the observed wind speed in J15. Surface energy fluxes and

the large-scale subsidence are prescribed as constants according to Ackerman et al. (2009) who focus on a similar stratocumulus base based on stratocumulus clouds observed in comparable conditions in a similar regime. The fluxes of latent and sensible heat are set as 93 W m^{-2} and 16 W m^{-2} , respectively, while the subsidence is described by the divergence of horizontal winds set as $3.75 \times 10^{-6} \text{ s}^{-1}$. The model grid resolution is set to 50 m (10 m in the vertical) and the domain size is 5 km across laterally, extending up to 1400 m in the vertical. A damping layer is applied in the top 100 m of the model grid to prevent unwanted wave propagation. The model timestep is 1 s.

The initial aerosol size distribution is described in the model as a sum of lognormal modes. J15 reported the accumulation mode aerosol concentration in the range of 200 to 800 cm^{-3} , with CDNC cloud droplet number concentration (CDNC) approximately $150 - 200 \text{ cm}^{-3}$. Therefore, we set the initial accumulation mode concentration to 200 cm^{-3} . Additional 400 cm^{-3} particles were allocated in the Aitken mode, which can be viewed as a typical feature in marine boundary layer (e.g. Zheng et al., 2018). However, for the current setup, the Aitken mode particles reside mostly below the critical size for droplet activation – pilot test runs showed little sensitivity in the results for the Aitken mode number concentration. In addition, natural GCCN particles consisting of sea salt, which are virtually omnipresent in marine boundary layers (Jensen and Nugent, 2017) and also seen by J15, were assigned to the background aerosol, with mode diameter at $1 \mu\text{m}$ and concentration at 1 cm^{-3} . The lognormal size distribution parameters for the initial model aerosol population are summarized in Table 1.

3.2 Cloud seeding

For the seeding aerosol, we use sea salt as a proxy for the particle composition. We use SALSA's parallel bin regimes to describe the seeding aerosol initially as externally mixed from the background. The seeding aerosol is then allowed to interact with the background particles through coagulation and cloud collection. We will assume two modes for the seeding particles, with mean diameters at $1.5 \mu\text{m}$ and $8 \mu\text{m}$, which roughly correspond to the mode mean diameters shown in J15, but are also more generally representative of the powdered salt size ranges presumed effective in terms of precipitation enhancement (Rosenfeld et al., 2010).

In the model experiments, the seeding emissions are performed in-cloud, near the cloud top altitude, at approximately 580 m, as in J15. Two methods for the release of the seeding particles are considered: i) a domain-wide instantaneous injection of the aerosol at the specified layer and ii) an explicit Lagrangian point source emission. In the former, the particles are assumed to occupy a layer of 50 m in depth. This seeding method does not represent a realistic scenario and serves to provide additional information about the importance of the total emitted mass in terms of the magnitude of the seeding effect. For the latter, the trajectory and speed of the emission source are prescribed for a more realistic seeding scenario. We assume the seeding aerosol plume to immediately occupy a cross-sectional area of $50 \times 50 \text{ m}^2$. Further dilution of the plume is controlled dominantly by grid-scale mixing. To mimic the airborne emissions, we assume a speed of 60 m s^{-1} for the source, whose trajectory is illustrated in Figure 3.3. The seeding source propagates towards the positive x-direction along a trajectory that covers the entire extent of the domain in y-direction. Since the seeding proceeds against the horizontal wind (in x-direction), the seeding is stopped at the middle of the domain. This is to avoid seeding the same plume twice, because the rear of the plume is advected back into the domain from the right due to the cyclic boundary conditions.

155 3.3 Model experiments

Our experimental strategy is to create two parallel sets of realizations: a control simulation without seeding (referred to as Ctrl) and a set of experiments with seeding particle emissions. This allows to account for both the direct microphysical effects, as well as the dynamical feedbacks potentially caused by the aerosol perturbation. We must take care, that the initial states for the control simulations and sensitivity seeding experiments are identical. Therefore, a “master” model run is performed, from 160 which the model state is saved to a “restart” file prior to the time of the seeding procedure. The length of the “master” run is 4 hours, to allow the boundary-layer mixing and precipitation process to settle in a quasi-steady-state (i.e. spinup). All our model experiments, including both the control and seeding experiments, are initialized from this restart file, which ensures that any differences in the experiments can be attributed directly to the seeding.

The main model experiments performed in this study are summarized in Table 2. The seeding experiments Seed1 and Seed2 165 use the moving point emission source along the trajectory shown in Figure 4.3. The total seeding rate in the former experiment is set as $1.5 \times 10^{11} \text{ s}^{-1}$ and in the latter as $1.5 \times 10^{12} \text{ s}^{-1}$. With the assumed initial injection plume cross-section and the aircraft speed, this yields an initial plume concentration initial concentrations of approximately 1 cm^{-3} and 10 cm^{-3} , respectively, which will be rather quickly diluted by in-cloud mixing and drizzle formation. These settings were chosen in terms of the seeding particle concentrations in the mixed plume, as it depends strongly on the assumed injection cross-section. We set the 170 target concentration after mixing to be similar to the estimated range in J15 (10^{-4} to 10^{-2} cm^{-3}), as shown in Section 4. Please note that while the injection procedure in Seed1 and Seed2 tries to mimic the aircraft emission, we do not consider e.g. the possible aerodynamic effects caused by the aircraft. In the experiment Seed3 the seeding particles are injected instantaneously 175 in a domain-wide slab at the same altitude as the point emissions in Seed1 and Seed2. The initial concentration in Seed3 is set as 1 cm^{-3} . Comparing the model results between the point source and domain slab emissions and different emission rates helps to understand the impact of the total emitted mass to

In addition to the main experiments, a small ensemble of sensitivity tests is performed based on the Ctrl and Seed2 configurations, where we vary the boundary layer moisture content and the efficacy large-scale divergence settings between the ensemble members randomly within $\pm 10\%$ of the values used in the corresponding main experiments. The ensemble has 180 20 members (i.e. pairs of simulations with the Ctrl and Seed2 configurations), whose purpose is to characterize the sensitivity of the seeding, since it critically affects the concentration in the diluted population. Note, that we do not consider the possible aerodynamic effects caused by the aircraft results to the model initial conditions. The data is used to investigate process rate statistics as well, which tend to be highly variable in space and time. However, these sensitivity tests obviously do not provide an exhaustive representation of the different sensitivities of the seeding process, which should be tackled with dedicated research.

3.4 Sensitivity of precipitation

185 The overall precipitation rate in the simulated case is rather low. The overall rather low both in model and observations: the observed estimate reported in J15 is about 0.05 mm h^{-1} 0.04 mm h^{-1} on average, sampled around the cloud base height. In order to evaluate the seeding efficacy estimate the significance of the seeding effects in UCLALES-SALSA relative to the

findings in J15, we want to match the simulated precipitation rate as close as possible to the measurements. We find that in the current case, the precipitation rate is strongly controlled by ~~two~~three key aspects in the model setup: the background aerosol and the vertical resolution. ~~In case of~~ and the prescribed subsidence rate. For the former, we focus here on the role of natural GCCN, due to their overall small concentration, but potentially strong impact on drizzle formation. For the latter, ~~middle, the~~ vertical resolution of the model is known to have a substantial influence on the representation of entrainment mixing at cloud top (Stevens et al., 2005). This is expected to modulate the rate of evaporation of cloud droplets due to the entrained dry air from above the cloud, which affects the mean droplet size and the size distribution width and, therefore, drizzle formation via the collision-coalescence process. Lastly, the subsidence rate is known to impact precipitation formation due to effects on cloud thickness and, thus, droplet growth (Chen et al., 2011). Pilot model simulations are performed to test the corresponding choices made in our simulation setup.

First, Figure 4-4 illustrates the effect of GCCN concentration on the simulated precipitation in pilot experiments. With 1 cm^{-3} (used in the experiments), we obtain a precipitation rate much closer to the observed estimate, than with a lower concentration (0.1 cm^{-3}). Similar concentrations of GCCN were also measured in the field campaign according to J15 and the good agreement with the observed precipitation rate (0.05 mm h^{-1} ~~0.04 mm h^{-1}~~) warrants the use of the background aerosol size distribution detailed in Table 1.

Second, Figure 5-5 shows the effect of vertical resolution on the simulated precipitation rate. It is evident, that 20 m spacing in the model vertical grid yields lower precipitation rate, than the simulations with 5 m or 10 m grid spacings. That said, the difference seen between 5 m and 10 m grid spacings is minor. Even though 10 m resolution has been shown to be inadequate to fully represent the effects of e.g. entrainment mixing (Stevens et al., 2005), considering this result and the fact that the UCLALES-SALSA is computationally a rather expensive model, we find that the 10 m vertical grid spacing is justified.

Third, Figure 6 presents the precipitation rate with the large-scale divergence rate selected for our simulations ($3.75 \times 10^{-6} \text{ s}^{-1}$; Ackerman et al., 2000) and a higher value representing stronger subsidence ($8.0 \times 10^{-6} \text{ s}^{-1}$, as in Chen et al., 2011). The results indeed indicate that the precipitation rate is quite sensitive to the subsidence, similar to Chen et al. (2011), and that the lower setting yields precipitation rates much closer to the measurements reported in J15.

4 Results

4.1 ~~Precipitation fluxes~~Seeding effects on precipitation and cloud properties

Figure 6-7 shows the flux of precipitating water sampled at an altitude of 300 m, which is close to the cloud base height (~~around 250 m after the seeding~~). In the control case, the precipitation rate is approximately $0.03 - 0.05 \text{ mm h}^{-1}$, which agrees well with the corresponding measured precipitation rate in J15. It is evident, that the seeding emission rate and seeding strategy have a strong influence on the seeding efficiency. The experiment Seed1 (with a low emission rate) yields a positive, but a rather weak signal in terms of the precipitation flux. Instead, Seed2 (with high emission rate) approximately doubles the precipitation flux within an hour after the start of the seeding, as compared to the control run. Likewise, even stronger (by a factor of 3) increase in precipitation is shown by Seed3, where the ~~seeding rate initial seeding concentration~~ is the same as in Seed1, but

the total injected mass is much larger because it is applied to all grid points across the target layer. Therefore, it is important to consider the impact of the seeding strategy on the ~~diluted mixed~~ plume concentration.

Figure 7-8 shows the estimated domain mean profiles of the seeding particle concentration. Since the seeding takes place in-cloud, practically all the particles are activated very quickly. Therefore, the concentration is ~~analysed~~ ~~analyzed~~ as the number of cloud droplets formed by the seeding particles, 15 minutes after the seeding. This gives the plumes some time to ~~dilute~~ ~~mix~~; with further delay, the plume concentration starts to be more and more affected by precipitation, after which it is difficult to robustly distinguish the particles associated with seeding in our modelling setup. Moreover, taking the profile as domain average is justified because the trajectory of the source in Seed1 and Seed2 is set to cover the entire width of the domain in y direction, as depicted in Figure 33, and it ~~does not take long~~ ~~takes approximately 10-15 minutes after the seeding injection~~ for the turbulent diffusion to spread the seeding ~~particles~~ across the domain area. As indicated ~~in Figure 7~~ ~~in Figure 8~~, clearly the highest average concentration is seen for Seed3 and the lowest for Seed1, which indeed emphasizes the connection between the ~~diluted plume concentration to the seeding efficacy. Therefore, as Figure 7 suggests, plume concentration and the seeding effects. The mean of the Seed2 profile in Figure 8 suggests that~~ in order to produce an approximately 2-fold precipitation yield, the concentration ~~in the diluted plume of~~ of seeding particles mixed in the cloud layer should be on the order of 0.01 cm^{-3}

As briefly discussed in Section 3.4, modelling precipitation is sensitive to various aspects of the model setup and the initial conditions, which yield uncertainties in the simulations. These uncertainties are thus part of the estimated seeding effects as well, which we test based on the ensemble simulations performed using the Ctrl and Seed2 configurations, varying the input boundary-layer moisture content and the large-scale subsidence rate. Figure 9 shows the absolute and relative precipitation enhancements between the two model configurations for each ensemble member. The seeding effects are somewhat sensitive to the boundary-layer moisture content, with the absolute precipitation enhancement increasing with increasing moisture (and the overall precipitation rate). In terms of the relative enhancement, the conclusion is nearly opposite, with the largest relative enhancement seen with the driest boundary-layer (associated with low precipitation rates). Considerably less sensitivity is found to varying subsidence within the $\pm 10\%$ range, although the precipitation rate did show sensitivity to larger changes in subsidence (Figure 6).

Looking at the general cloud properties shows that the model simulations tend to overestimate the liquid water content (LWC) compared to the observed values: as indicated in Figure 10, the simulated LWC is around the $0.14 - 0.15 \text{ g m}^{-3}$ range near the cloud base, while the corresponding estimate in J15 is 0.09 g m^{-3} . However, both our simulations and the reports in J15 indicate quite substantial variability in these values and the result varies strongly depending on how deep into the cloud layer the sampling is performed. The layer at 300 m is chosen for sampling, which is close to cloud base but remains consistently in-cloud. Figure 10 suggests an increasing reduction in LWC with increasing seeding emission, which is qualitatively in agreement with the findings in J15. Further, the simulated CDNC shown in Figure 11 is within the range, albeit slightly above the mean, reported by J15 around the time of the seeding (simulated mean approximately 180 cm^{-3} vs the observed mean 162 cm^{-3}), although, again the variability is substantial in both estimates. The model CDNC shows a decreasing slope, which we attribute mainly to cloud processing and the gradual scavenging of the CCN particles (there is no replenishment of aerosol in our simulations). The seeding experiments show a clear decrease in CDNC as compared to the Ctrl

configuration. However, in the model the effect is not as strong as the decrease reported in J15 (i.e. from 162 cm^{-3} to 77 cm^{-3} near cloud base).

4.2 Microphysical signatures

The main hypothesized pathways to precipitation enhancement via hygroscopic seeding in warm low-level clouds include 1) the reduction of CDNC due to increased competition for water vapor induced by the large seeding particles and 2) enhanced collision-coalescence (Segal et al., 2004; Rosenfeld et al., 2010). Thus, to better understand the reasons for the simulated enhanced precipitation enhancement shown in Figure 67, we will analyze more closely the cloud microphysical effects induced by the seeding.

To start with, our model shows very little change in the in-cloud relative humidity supersaturation between the experiments. This is in line with releasing the seeding aerosol close to the cloud top height, following the experimental approach in J15. Consequently, since, as shown in Figure 12, sampled 15 minutes after seeding. As most of the ambient aerosol are activated close to the cloud base at the level of peak supersaturation close to the cloud base, the the peak supersaturation, Figure 12 gives the first indication that the seeding effect through water vapor competition effect appears to be minor is likely of minor importance in our simulations. However, the simulated cloud droplet number concentration does show a decrease (Figure 8) In order to find proof for this, we analyze the microphysical process rates. The process rates exhibit substantial spatial and temporal variability, so they are analyzed using the ensemble simulations, taking the mean across the ensemble members. Figure 13 shows the ensemble mean relative changes between the Ctrl and Seed2 configurations for the rates of cloud activation, autoconversion and accretion. Note that the latter two are calculated directly by the coagulation scheme of UCLALES-SALSA and therefore the rates are diagnosed during model runtime as the water mass transferred from cloud droplet bins to drizzle/precipitation bins, and as the mass collected by the drizzle and rain drops from other liquid droplet size classes, respectively. Consequently, since these processes are not described by dedicated parameterizations in our model, the corresponding rates are most likely not directly comparable with results from other microphysics schemes that do employ dedicated parameterizations. Nevertheless, Figure 13 generally corroborates the interpretation suggested by the supersaturation profiles: the cloud activation rate shows only a modest decrease (by up to 6 %), which we consider as a sign of enhanced is gradually enhanced over the course of 2-3 hours (almost until the end of the simulation). The gradual change hints that instead of a direct seeding effect via the water vapor competition, the difference is most likely caused by the enhanced scavenging of CCN particles between the Ctrl and Seed2 configurations. In contrast, the autoconversion rate shows a substantial and sharp increase at the time of the seeding (up to 30 %), which lasts for about half an hour. Afterwards, the accretion rate shows an increase of comparable magnitude, which indicates that after the peaked autoconversion rate, the effect of seeding is shifted from the collision-coalescence due to the injection of large CCN particles. Again, the reduction in CDNC is most pronounced for the highest seeding aerosol emissions, i.e. the experiments Seed2 and Seed3. The strongest reduction is seen in the latter, with a difference by almost 10 % compared to the control case mode between cloud droplets to more of a droplet collection type of growth mode controlled by the existing drizzle-sized droplets and rain. The latter also shows a prolonged effect seen

until the end of the simulation. Therefore, enhanced collision rate between droplets is most likely the main pathway for the seeding induced precipitation enhancement according to the model results.

More evidence is provided by plotting out details on the effects of seeding on the cloud microphysical properties are obtained by plotting the hydrometeor size distributions in the seeding experiments before and after the time of the seeding emission in Figure 9–14. The size distributions are sampled in-cloud at 300 m altitude, close to the cloud base height. While the size distributions show negligible changes in the experiment Seed1, in Seed2 and Seed3 there is clearly an increase in the concentration of droplets around the $100 \mu\text{m}$ – 100 – $200 \mu\text{m}$ size range after seeding. After 1 hour, there is also a definite increase in the concentration of larger hydrometeors ($> 500 \mu\text{m}$), pointing out the time needed for the seeding induced drizzle drops to grow to rain drop sizes by collection processes. In particular, these simulated size distributions, and the effects of seeding therein, bear a remarkable resemblance to the features in the measured size distributions at the corresponding altitude presented by These features are similar to the corresponding observed size distributions presented in J15; the modelled seeding appears to reproduce the observed effects on the droplet population very closely at the correct size ranges. We consider this to be a very strong argument in support of the ability of: similar to Figure 14, the observed size distributions showed a clear increase in concentrations around the 100 – $200 \mu\text{m}$ range as well as in the sub-millimeter diameters after the seeding. The former corresponds to the expected size range for the transition between cloud droplets and drizzle. This is accompanied by a shoulder in the decreasing slope of the distribution both in the model as well as in the observations in J15. Here we find slight differences between the model and observations: in UCLALES-SALSA the transition range is found just below $100 \mu\text{m}$ whereas in J15 it appears to be closer to $200 \mu\text{m}$. This also yields a difference in the magnitude of the seeding effect, which seems to be larger in J15. In addition, looking at the distribution slope for cloud droplets, UCLALES-SALSA indicates a slightly more peaked distribution shape than the observations in J15. The more peaked shape is speculated to arise from the strategy for the cloud droplet bin representation chosen in UCLALES-SALSA (described in Section 2). Nevertheless, the marked qualitative similarity between the model seeding effects and the results in J15 is a very encouraging result and provides strong support for UCLALES-SALSA being able to capture the primary microphysical pathway in how the seeding aerosol affects the precipitation rate for the hygroscopic seeding effects on precipitation in the case examined.

To close the connection between the microphysical effects and precipitation, Figure 10–15 shows the contribution to the overall precipitation flux as a function of size. The data in Figure 10–15 is obtained from the same height level as in Figure 9–14. As expected, enhanced precipitation due to seeding first takes place by the drizzle size ranges (about $100 \mu\text{m}$) and later by the growth of the larger rain drops. The latter is strongly associated with the peak precipitation flux seen just after 5 hours (model time) in Figure 6–1–1.5 hours after the seeding emission in Figure 7, especially in the experiments experiment Seed3.

5 Discussion and conclusions

The coupled LES-aerosol-cloud model UCLALES-SALSA was used to study the precipitation enhancement by hygroscopic seeding in marine stratocumulus clouds. Results from field observations reported in J15 were used as the basis for a series of model experiments performed to map the dependency of precipitation enhancement on between precipitation enhancement and

the rate of seeding aerosol emission and the injection strategy. The simulation time period was matched with the observations together with the initial thermodynamic profiles and the ambient aerosol size distributions.

325 ~~The overall simulated precipitation rates and cloud properties were in good agreement with the results reported in J15, and the simulated mean precipitation flux was approximately $0.03 - 0.05 \text{ mm h}^{-1}$ near the cloud base.~~ Our approach to estimate the effects of seeding was to compare the results between a control run (without seeding) and experiments with seeding, in which the seeding emissions were described both by a moving point emission source and by direct injection of particles to a domain-wide slab. Care was taken to keep the model initial state and the boundary conditions identical between the control run and seeding experiments, so that differences between the simulations could be attributed directly to the seeding aerosol.

330 ~~Our results show up to 2-3 fold increase in the precipitation flux sampled at cloud base altitude, depending on the experiment. This is comparable to~~ The overall simulated precipitation rates in the control run were in good agreement with the results reported in J15 with the mean of approximately 0.04 mm h^{-1} sampled close to the cloud base. Cloud properties produced by the model were also found mostly in the observed range according to J15, although some overestimation was seen in the mean LWC before the seeding. For CDNC the model indicated a decreasing trend in the domain mean during the simulation, 335 which we attributed mainly to cloud processing and scavenging, since the aerosol was not replenished during the simulation. The clouds (and precipitation) were seen to be somewhat sensitive to model initial and boundary conditions, some of which were prescribed as fixed values (e.g. surface fluxes and large-scale subsidence), which adds a degree of uncertainty in the model results. Nevertheless, the values chosen for the simulations produced a consistent set of cloud properties that were in reasonable agreement with the results in J15. ~~In successful cases, the seeding produces~~

340 Regarding the seeding effects, the model produced up to 2-3 fold enhancement in the precipitation flux, where the magnitude was found to scale with the total emitted mass of the seeding aerosol. This enhancement is slightly weaker than that reported by J15 (up to 4-fold enhancement). The model seeding produced a somewhat sustained effect ~~for up to 2-3 hours after the seeding initialization~~ lasting until the end of the simulations, with the peak enhancement visible within approximately 1-1.5 hours time ~~in Seed3 and around 2 hours in Seed1 and Seed2~~. However, ~~our results suggest, it was determined~~ that the minimum 345 concentration in the seeding particle plume, after allowing it to ~~dilute mix~~ within the cloud layer, should be rather high, on the order of ~~$0.01 \text{ cm}^{-3} 10^{-2} \text{ cm}^{-3}$~~ , in order to generate an approximately 2-fold precipitation enhancement. This concentration is on the high end of the diluted plume ~~concentrations~~ concentration range estimated by J15 ~~-(from 10^{-4} to 10^{-2} cm^{-3})~~.

350 ~~To increase the confidence to our results, It was determined that the seeding effects in the model mainly arise via the enhanced collision-coalescence and droplet collection rates. Support for this interpretation was found by analyzing the cloud microphysical properties and process rates. The model showed only minor effects on the RH after the seeding and minor changes in the cloud droplet activation rate, which suggests that the hypothesized seeding effect via water vapor competition affecting the cloud droplet number is of minor importance in the simulated case. This agrees with the conclusions in Rosenfeld et al. (2010), although their work focused on more convective cloud types. In contrast, the drizzle production (i.e. autoconversion) and accretion rates showed a more significant enhancement emerging immediately after the seeding injection (the latter sustained until the end of the simulation, i.e. 3 hours after seeding) by up to 30 – 35 %. Thus, the results suggest a dominant role for the enhanced collision processes in this case. The seeding aerosol was released close to cloud top in the model simulations,~~

following the experimental approach in J15. It is possible this would act to reduce the seeding effects via water vapor competition and cloud activation compared to a different strategy of injecting the particles at cloud base, even though the seeding particles are getting mixed and sedimented to the lower parts of the cloud in the current experiments as well. Moreover, 360 since UCLALES-SALSA solves the condensation equations in a size-resolving framework, the model has the technical ability to describe the competition for water vapor due to particle growth between the seeding aerosol and the ambient cloud droplets not only at cloud base, but in other parts of the cloud as well. Since we do not find clear signs of such effects in the model data, they are likely limited by the relatively low seeding particle concentrations and masked by other in-cloud variability, although 365 being theoretically feasible. The significance of the different seeding effects potentially depends also on the presence of natural GCCN aerosol in the background, as suggested by e.g. parcel model calculations (Segal et al., 2004). GCCN are expected to be found in marine boundary-layers (Bian et al., 2019) and were thus included in the model experiments in the current work.

Further analysis of the cloud microphysics showed that the model simulations reproduced the ~~simulated seeding effects on the cloud microphysical properties were inspected. The model simulations skillfully reproduced the main features of the observed~~ seeding effects on the hydrometeor size distribution, as compared with J15. The model size distributions indicated 370 a temporal propagation of increased concentrations first in the drizzle size range and later towards the larger rain drop sizes, which was expected as the result of an enhanced collision growth of droplets. ~~Accordingly, the model also showed a decrease in the total CDNC by up to 10 % due to the seeding emissions~~ While assessing the process pathways for seeding effects represented by UCLALES-SALSA, the similarities seen in the droplet size distributions between the model and observations was found particularly encouraging.

375 The impact of seeding on other cloud properties was qualitatively similar to the results in J15, i.e. both LWC and CDNC were decreased. The magnitude of the effect increased with the total mass of the injected seeding aerosol. However, ~~again the notable micropysical effects only become visible with the aforementioned 0.01 cm^{-3} diluted seeding plume concentration. In addition, J15 reported a somewhat larger decrease in CDNC after the seeding as with the precipitation rate, the seeding effects on the cloud properties in the model were clearly weaker than those reported for the observations. Arguably, estimating the seeding efficacy analyzing the seeding effects~~ from the model by comparing multiple realizations provides a more robust estimate (~~at least~~ in terms of the data sampling) than estimating the effects of seeding aerosol from temporally consecutive sets of observations. Given the qualitatively very similar seeding effects between the observations and our model, but a larger decrease in CDNC in the observations than in our model, we speculate that other factors than the seeding alone might be playing 380 a role in the observed cloud layer. ~~These include possible meteorological variations~~ An example would be the aforementioned gradual decrease in CDNC seen in the model simulations, which was further enhanced by seeding. One can speculate that a single model realization would therefore have resulted in an overestimation of the seeding effect. Unfortunately however, we 385 can not prove that the decreasing trend in CDNC is a realistic feature for this particular case. The model experiments are also subject to a number of other uncertainties that may enhance or suppress the seeding effects and therefore contribute to the differences seen with the observations. The uncertainties arise from both the description of initial and boundary conditions, and from the model numerics. In particular, tests with varying initial and boundary conditions indeed showed that the model 390 seeding effects are quite sensitive to parameters such as the initial thermodynamic profiles and the prescribed large-scale

subsidence. Physically, this reflects the impact of changing the boundary-layer and cloud dynamics on the susceptibility of stratocumulus clouds to changes in CDNC and aerosol, in this case particularly the seeding particles. Potential deficiencies in the description of the dynamical and thermodynamical environment may therefore result in the weaker seeding effects as

395 compared to observations. Moreover, by the same argument, the results presented here are most likely not well generalized to different environments. From a more technical perspective, the variability in the seeding effects illustrated by the sensitivity tests reflects the model uncertainties in UCLALES-SALSA that arise from the numerical representation of the particle size distributions as well as from deficiencies in the parameterized process descriptions. In addition, some specific aspects of the simulated case are currently not included the model: we did not account for possible aerodynamic effects from the aircraft used
400 for seeding, which we do not account for in our simulations. The latter has been studied in the context of ice and mixed-phase clouds (Kärcher, 2018; Moisseev et al., 2019), but in terms of warm cloud seeding, a dedicated study would be required.

Despite the uncertainties, which are not unique to UCLALES-SALSA but present in all modelling studies, the results of this work give a quite consistent view into the seeding process pathways, with several characteristics at least qualitatively
405 very similar to the observations in J15. Therefore, the highly detailed description of microphysics by the SALSA module in conjunction with the cloud resolving framework by UCLALES provides a useful tool for continued investigation of the potential for precipitation enhancement by cloud seeding. Flare burning is a commonly used and cost effective method to produce the seeding particles, but they have the tendency to produce particles in a wide range of sizes, with significant contribution from sub-micron particles. Our results highlight the importance of the seeding plume concentrations. Even though the plume
410 concentration can be controlled to an extent both by the emission rate as well as the seeding strategy (e.g. flight plan, use of multiple aircraft), the results corroborate the view presented in recent literature (Rosenfeld et al., 2010), that obtaining a high enough concentration of large ($> 1 \mu\text{m}$) CCN from flares in terms of efficient precipitation enhancement might be challenging with currently used practical applications.

Code availability. The model source code is freely available at Github: <https://github.com/UCLALES-SALSA/UCLALES-SALSA>

415 *Author contributions.* JT and AA share an equal contribution in performing and analysing model experiments, and for writing most of the paper. JT, TR, SR, and H Kokkola are the main contributors in developing the UCLALES-SALSA code. H Korhonen, H Kokkola and SR took part in evaluating the model results and writing the paper.

Competing interests. The authors declare no conflict of interests.

Acknowledgements. This material is based on work supported by the National Center of Meteorology, Abu Dhabi, UAE under the UAE Research Program for Rain Enhancement Science. The work was also supported by the Academy of Finland (project numbers 283031, 309127, 322532, and the Centre of Excellence in Atmospheric Science, 272041) and the European Research Council (project ECLAIR, 646857).

References

Ackerman, A. S., van Zanten, M. C., Stevens, B., Savic-Jovicic, V., Bretherton, C. S., Chlond, A., Golaz, J.-C., Jiang, H., Khairoutdinov, 425 M., Krueger, S. K., Lewellen, D. C., Lock, A., Moeng, C.-H., Nakamura, K., Petters, M. D., Snider, J. R., Weinbrecht, S., and Zulauf, M.: Large-Eddy Simulations of a Drizzling, Stratocumulus-Topped Marine Boundary Layer. *Mon. Weather Rev.*, 137, 1083–1110, doi:10.1175/2008MWR2582.1, 2009.

Bian, H., Froyd, K., Murphy, D. M., Dibb, J., Darmenov, A., Chin, M., Colarco, P. R., da Silva, A., Kucsera, T. L., Schill, G., Yu, H., Bui, P., 430 Dollner, M., Weinzierl, B., Smirnov, A.: Observationally constrained analysis of sea salt aerosol in the marine atmosphere. *Atmos. Chem. Phys.*, 19, 10773–10785, <https://doi.org/10.5194/acp-19-10773-2019>, 2019.

Bigg, E. K.: An independent evaluation of a South African hygroscopic cloud seeding experiment, 1991–1995. *Atmos. Res.*, 43, 111–127, 1997.

Boutle, I., Price, J., Kudzotsa, I., Kokkola, H., Romakkaniemi, S.: Aerosol–fog interaction and the transition to well-mixed radiation fog, 435 *Atmos. Chem. Phys.*, 18, 7827–7840, <https://doi.org/10.5194/acp-18-7827-2018>, 2018.

Bruintjes, R.T.: A Review of Cloud Seeding Experiments to Enhance Precipitation and Some New Prospects. *Bull. Amer. Meteor. Soc.*, 80, 805–820, [https://doi.org/10.1175/1520-0477\(1999\)080<0805:AROCSE>2.0.CO;2](https://doi.org/10.1175/1520-0477(1999)080<0805:AROCSE>2.0.CO;2), 1999.

Cotton, W.R.: Modification of Precipitation from Warm Clouds—A Review. *Bull. Amer. Meteor. Soc.*, 63, 146–160, 440 [https://doi.org/10.1175/1520-0477\(1982\)063<0146:MOPFWC>2.0.CO;2](https://doi.org/10.1175/1520-0477(1982)063<0146:MOPFWC>2.0.CO;2), 1982.

Chen, Y.-C., Xue, L., Lebo, Z.J., Wang, H., Rasmussen, R.M., Seinfeld, J.H.: A comprehensive numerical study of aerosol-cloud-precipitation interactions in marine stratocumulus. *Atmos. Chem. Phys.*, 11, 9749–9769, <https://doi.org/10.5194/acp-11-9749-2011>, 2011.

Dadashazar, H., Wang, Z., Crosbie, E., Brunke, M., Zeng, X., Jonsson, H., Woods, R. K., Flagan, R. C., Seinfeld, J. H., Sorooshian, A.: Relationships between giant sea salt particles and clouds inferred from aircraft physicochemical data. *J. Geophys. Res. Atmos.*, 122, 3421–3434, doi:10.1002/2016JD026019, 2017.

Feingold, G., Cotton, W. R., Kreidenweis, S. M., Davis, J. T.: the impact of giant cloud condensation nuclei on drizzle formation 445 in stratocumulus: implications for cloud radiative properties. *J. Atmos. Sci.*, 56, 4100–4117, [https://doi.org/10.1175/1520-0469\(1999\)056<4100:TIOGCC>2.0.CO;2](https://doi.org/10.1175/1520-0469(1999)056<4100:TIOGCC>2.0.CO;2), 1999.

Flossmann, A. I., Manton, M., Abshaev, A., Bruintjes, R., Murakami, M., Prabhakaran, T., Yao, Z.: Review of advances in precipitation enhancement research. *Bull. Amer. Meteor. Soc.*, 100, 1465–1480, DOI: 10.1175/BAMS-D-18-0160.1, 2019.

Ghate, V. P., Albrecht, B. A., Kollias, P., Jonsson, H., Breed, D. W.: Cloud seeding as a technique for studying aerosol-cloud interactions 450 in marine stratocumulus. *Geophys. Res. Lett.*, 34, L14807, doi:10.1029/2007GL029748, 2007.

Glenke, S., Kostinski, A., Fugal, J., Shaw, R. A., Borrman, S., Stith J.: Cloud droplets to drizzle: Contribution of transition drops to microphysical and optical properties of marine stratocumulus clouds. *Geophys. Res. Lett.*, 44, 8002–8010, doi:10.1002/2017GL074430, 2017.

Jensen, J. B., Lee, S.: Giant sea-salt aerosols and warm rain formations in marine stratocumulus. *J. Atmos. Sci.*, 65, 3678–3694, 455 DOI:10.1175/2008JAS2617.1, 2008.

Jensen, J. B., Nugent, A. D.: Condensational growth of drops formed on giant sea-salt aerosol particles. *J. Atmos. Sci.*, 74, 679–697, DOI:10.1175/JAS-D-15-0370.1, 2017.

460 Jung, E., Albrecht, B. A., Jonsson, H. H., Chen, Y.-C., Seinfeld, J. H., Sorooshian, A., Metcalf, A. R., Song, S., Fang, M., Russell, L. M.: Precipitation effects of giant cloud condensation nuclei artificially introduced into stratocumulus clouds. *Atmos. Chem. Phys.*, 15, 5645–5658, doi:10.5194/acp-15-5645-2015, 2015.

Kokkola, H., Korhonen, H., Lehtinen, K. E. J., Makkonen, R., Asmi, A., Järvenoja, S., Anttila, T., Partanen, A.-I., Kulmala, M., Järvinen, H., Laaksonen, A., and Kerminen, V.-M.: SALSA – a Sectional Aerosol module for Large Scale Applications. *Atmos. Chem. Phys.*, 8, 2469–2483, doi:10.5194/acp-8-2469-2008, 2008.

Kuba, N., Murakami, M.: Effect of hygroscopic seeding on warm rain clouds – numerical study using a hybrid cloud microphysical model. *Atmos. Chem. Phys.*, 10, 3335–3351, <https://doi.org/10.5194/acp-10-3335-2010>, 2010.

Kärcher, B.: Formation and radiative forcing of contrail cirrus. *Nat. Commun.*, 9, 1824, doi:10.1038/s41467-018-04068-0, 2018.

Lehahn, Y., Koren, I., Altaratz, O., Kostinski, A. B.: Effect of coarse marine aerosols on stratocumulus clouds. *Geophys. Res. Lett.*, 38, L20804, doi:10.1029/2011GL048504, 2011.

470 Moisseev, D., Lautaportti, S., Alku, L., Tabakova, K., O'Connor, E. J., Leskinen, M., Kulmala, M.: Inadvertent localized intensification of precipitation by aircraft. *J. Geophys. Res. Atmos.*, 124, 2094–2104, <https://doi.org/10.1029/2018JD029449>, 2019.

Rosenfeld, D., Axisa, D., Woodley, W. L., Lahav, R.: A quest for effective hygroscopic cloud seeding. *J. Appl. Meteor. Climatol.*, 49, 1548–1562, <https://doi.org/10.1175/2010JAMC2307.1>, 2010.

Segal, Y., Khain, A., Pinsky, M., Rosenfeld, D.: Effects of hygroscopic seeding on raindrop formation as seen from simulations using a 2000-bin spectral cloud parcel model. *Atmos. Res.*, 71, 3–34, doi:10.1016/j.atmosres.2004.03.003, 2004.

475 Stevens, B., Moeng, C.-H., Ackerman, A. S., Bretherton, C. S., Chlond, A., de Roode, S., Edwards, J., Golaz, J.-C., Jiang, H., Khairoutdinov, M., Kirkpatrick, M. P., Lewellen, D. C., Lock, A., Müller, F., Stevens, D. E., Whelan, E., and Zhu, P.: Evaluation of Large-Eddy Simulations via observations of nocturnal marine stratocumulus. *Mon. Weather Rev.*, 133, 1443–1462, 2005.

Tonttila, J., Maalick, Z., Raatikainen, T., Kokkola, H., Kühn, T., Romakkaniemi, S.: UCLALES–SALSA v1.0: a large-eddy model with interactive sectional microphysics for aerosol, clouds and precipitation. *Geosci. Model Dev.*, 10, 169–188, <https://doi.org/10.5194/gmd-10-169-2017>, 2017.

480 WWAP (UNESCO World Water Assessment Programme): The United Nations World Water Development Report 2019: Leaving No One Behind. Paris, UNESCO, 2019.

Zheng, G., Wang, Y., Aiken, A. C., Gallo, F., Jensen, M. P., Kollias, P., Kuang, C., Luke, E., Springston, S., Uin, J., Wood, R., Wang, J.: Marine boundary layer aerosol in the eastern North Atlantic: seasonal variations and key controlling processes. *Atmos. Chem. Phys.*, 18, 17615–17635, <https://doi.org/10.5194/acp-18-17615-2018>, 2018.

Table 1. Lognormal size distribution parameters for the initial aerosol consisting of three modes (rows). D is the mode mean diameter, N is the mode concentration and σ is the geometric standard deviation.

D[μm]	N[cm^{-3}]	σ
0.022	400	1.2
0.12	200	1.7
1	1	1.7

Table 2. List of model experiments, including the seeding particle injection method and the lognormal size distribution parameters for seeding. Subscripts 1 and 2 refer to the two lognormal modes used for the seeding aerosol. D is the mode mean diameter, N is the mode concentration and σ is the geometric standard deviation.

Experiment	Seeding strategy	D ₁ [μm]	N ₁ [cm^{-3}]	σ_1	D ₂ [μm]	N ₂ [cm^{-3}]	σ_2
CTRL	Ctrl	N/A	-	-	-	-	-
Seed1	Point source	1.6	0.5	1.3	8	0.5	1.6
Seed2	Point source	1.6	5	1.3	8	5	1.6
Seed3	Full slab	1.6	0.5	1.3	8	0.5	1.6

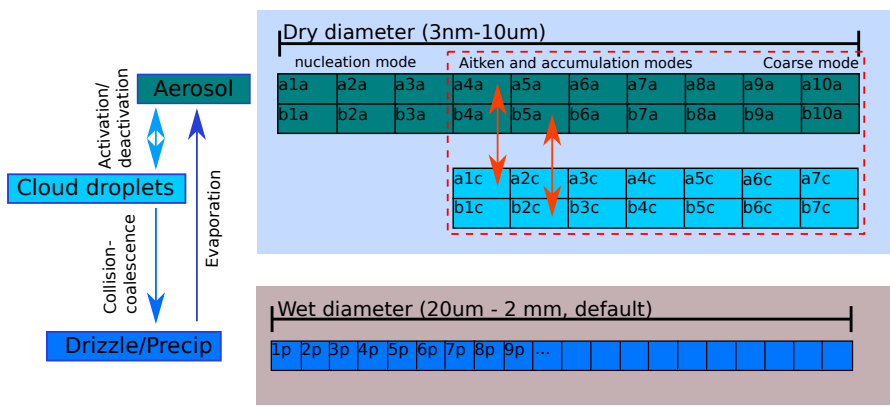


Figure 1. Schematic illustration of the microphysical interactions between the binned size distributions of different [particles](#) [particle](#) categories implemented in SALSA.

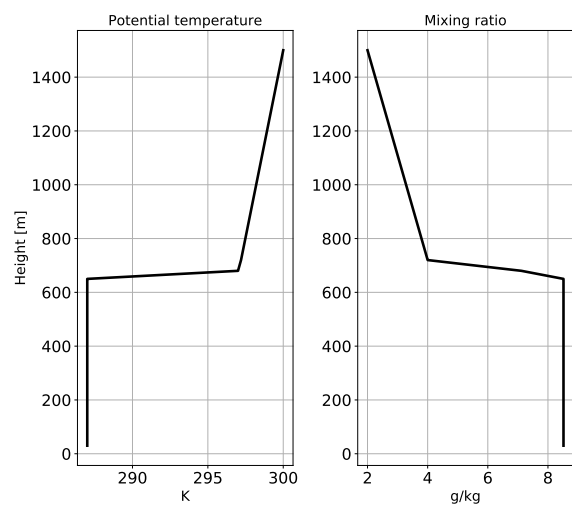


Figure 2. Input profiles of potential temperature and total water mixing ratio. The layer from approximately 300 m to 650m is saturated.

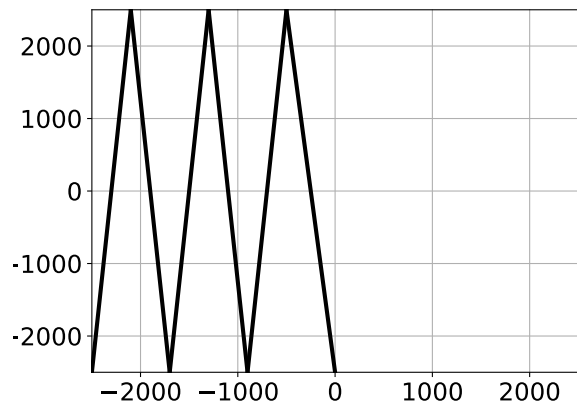


Figure 3. Trajectory of the cloud seeding emissions source on an x-y plane. The seeding starts from the lower left corner and progresses along the black line towards the positive x-direction.

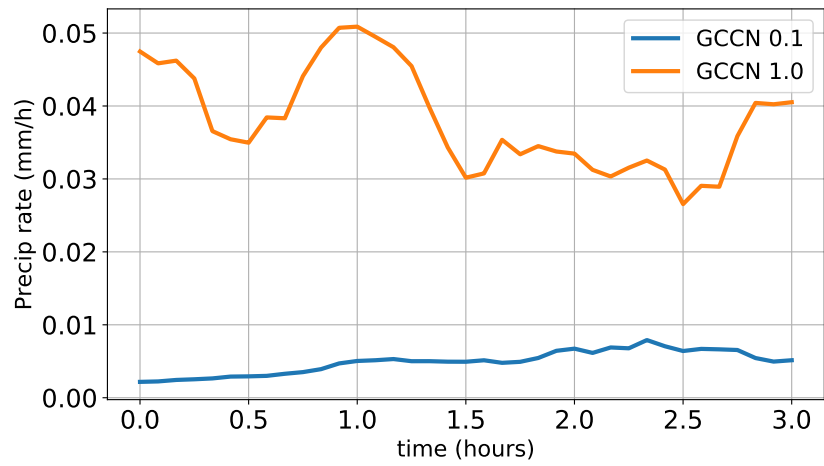


Figure 4. Effect of GCCN on precipitation rate close to cloud base (300 m). Precipitation rate is shown for low (0.1 cm^{-3} ; blue) and high (1.0 cm^{-3} ; orange) GCCN concentrations as a function of time (since the end of spinup).

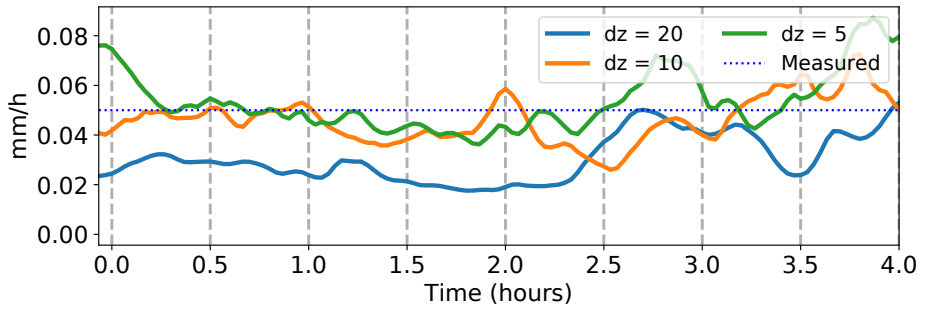


Figure 5. Effect of vertical resolution on the mean precipitation flux close to cloud base (300 m) as a function of time ([since the end of spinup](#)). The dashed blue line shows the corresponding precipitation rate estimated in J15.

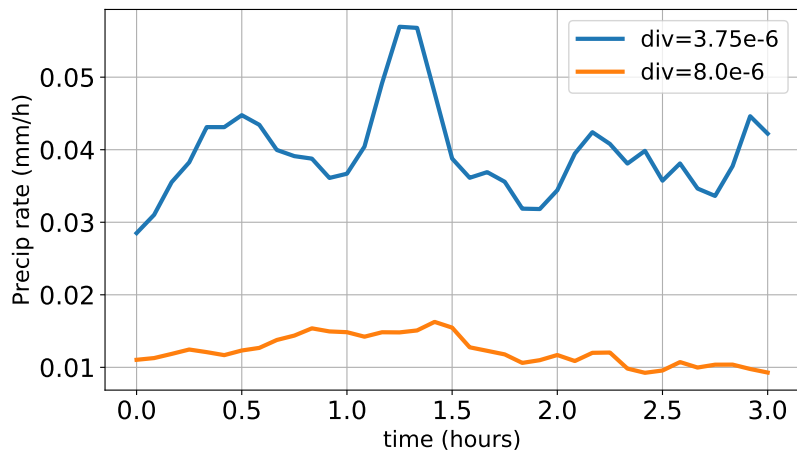


Figure 6. Domain Effect of large-scale divergence on the mean precipitation rate at close to cloud base (300 m) as a function of time in the control run and the seeding experiments. 0 hours time marks (since the start end of the seeding emission spinup).

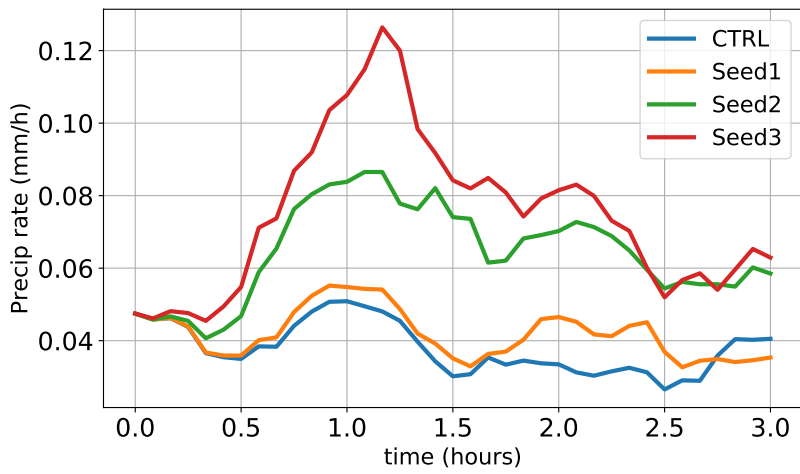


Figure 7. Domain mean precipitation rate at cloud base as a function of time since the seeding emission in the control run and the seeding experiments.

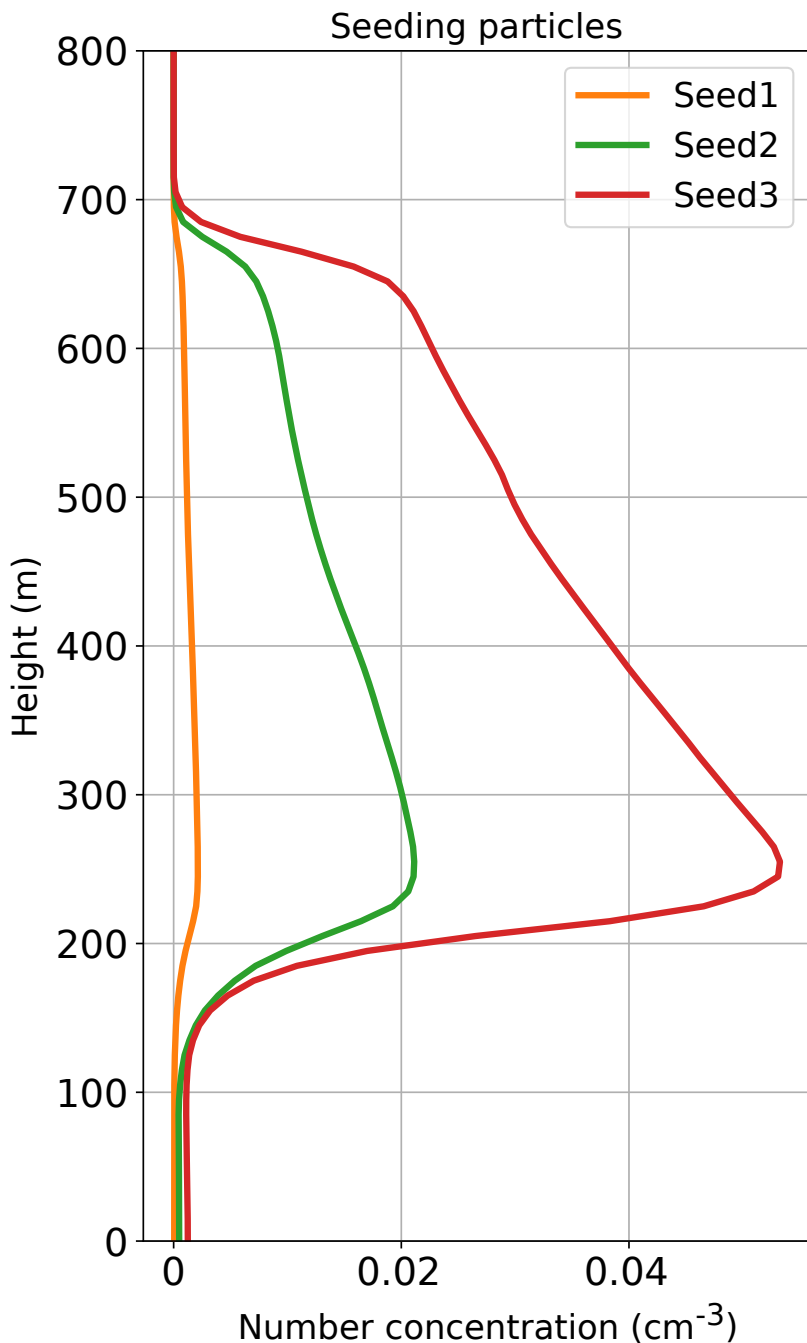


Figure 8. Domain mean profile of seeding particle concentrations 15 minutes after their release in the seeding experiments.

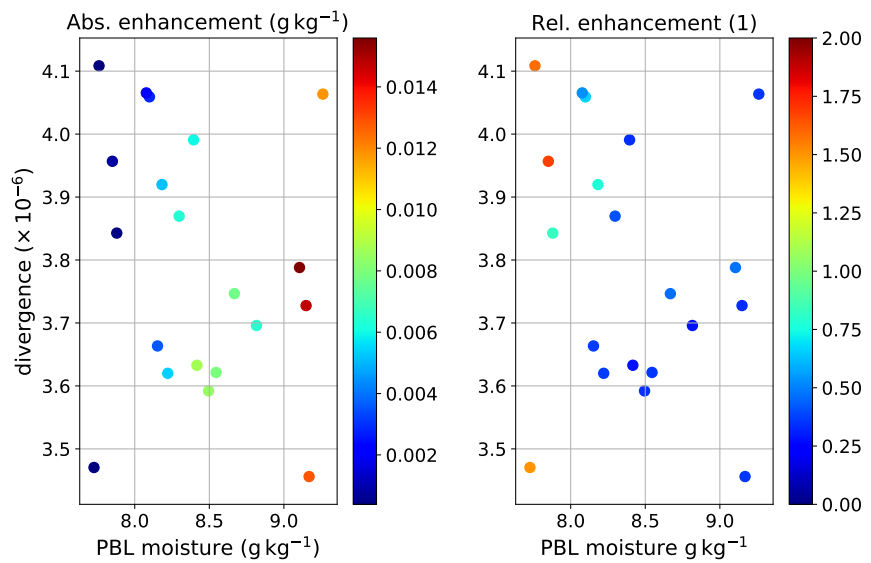


Figure 9. Precipitation enhancement (between the Ctrl and Seed2 configurations) in a simulation ensemble as a function of the prescribed large-scale subsidence and initial boundary-layer moisture content. The left panel shows the absolute enhancement, while the right shows the relative enhancement in the precipitation rate. The dots correspond to a domain mean in each ensemble member.

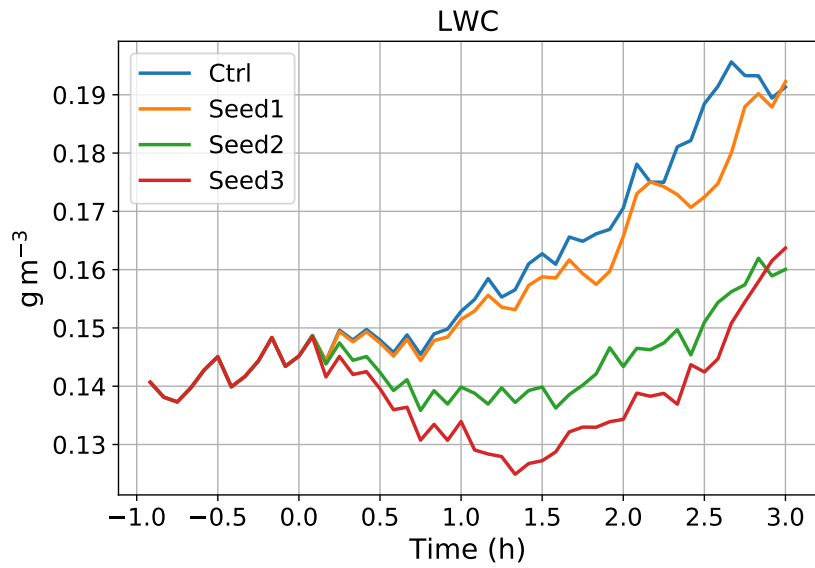


Figure 10. Evolution of the mean LWC in the Ctrl simulation and the seeding experiments sampled at 300 m height. The time on the x-axis is relative to the seeding injection time.

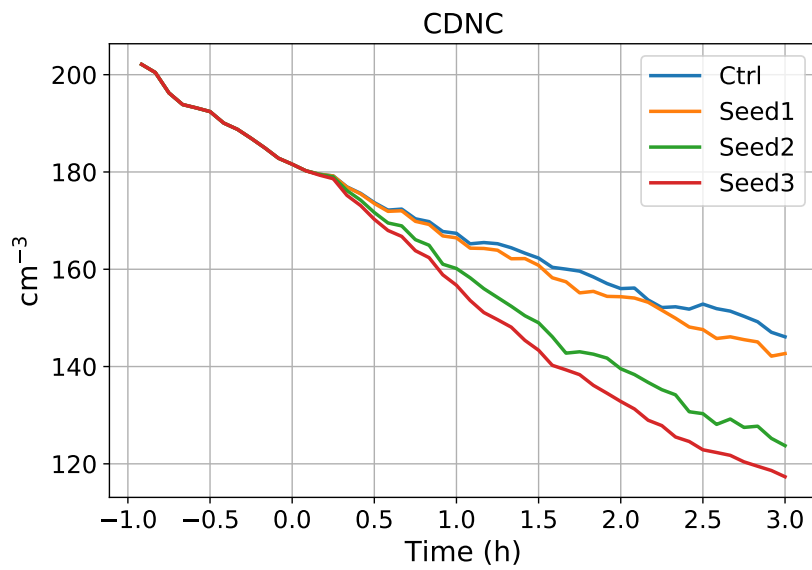


Figure 11. Evolution of CDNC in the Ctrl simulation and seeding experiments in a similar presentation to Figure 10.

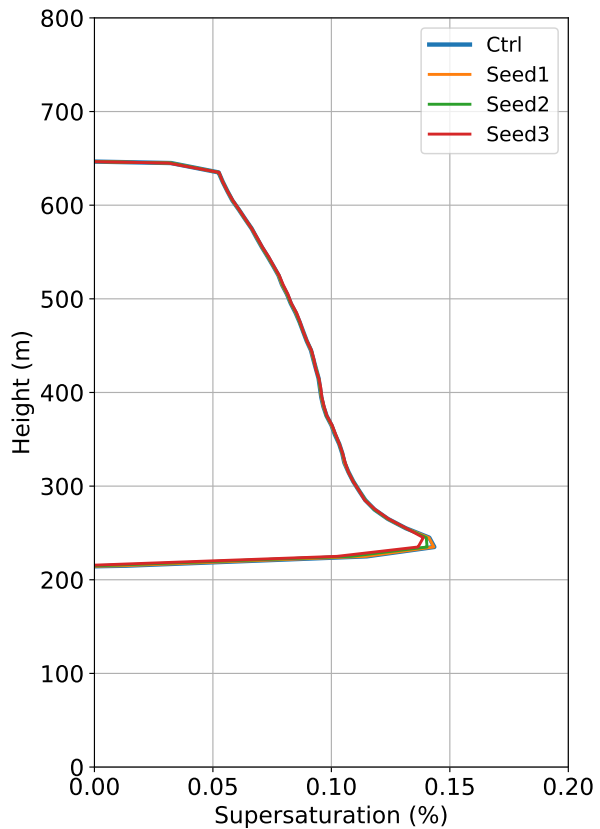


Figure 12. Vertical profiles of supersaturation averaged over areas of positive vertical velocity in the Ctrl simulation and seeding experiments 15 minutes after the seeding.

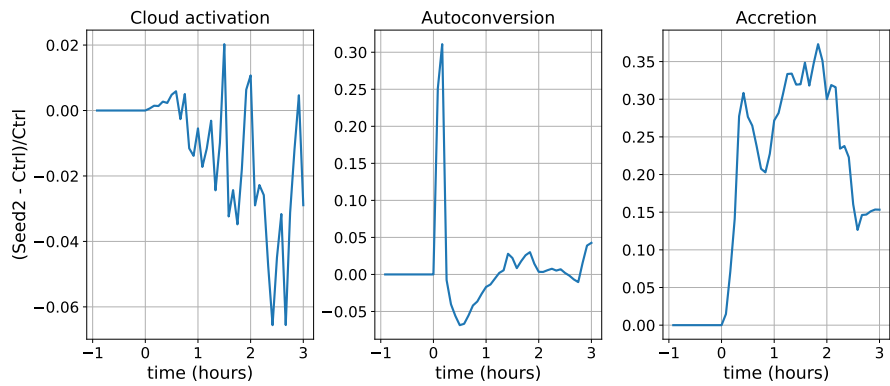


Figure 13. Domain mean cloud droplet number concentration 1 hour after the seeding time. Relative change in process rates between the control run **Ctrl** and **Seed2** configurations in per cent, calculated from the mean values taken across the ensemble simulations as a function of time (since the seeding experiments injection). Starting from the left, the panels show the change in cloud activation, autoconversion (drizzle formation) and accretion rates.

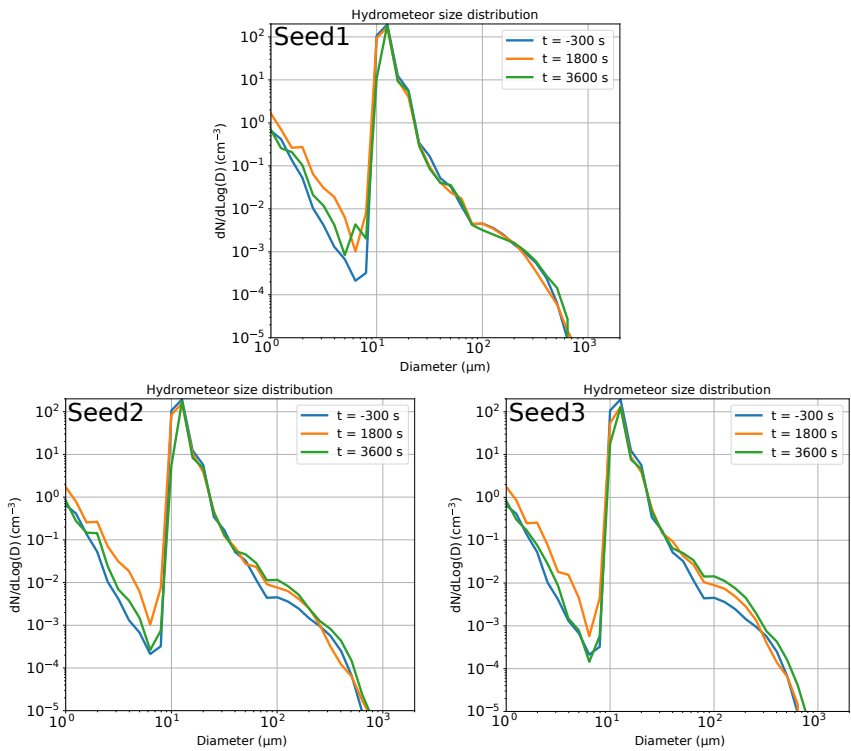


Figure 14. Hydrometeor size distributions close to cloud base (300 m altitude) before (-300 s) and after (1800 s and 3600 s) the particle injection in the seeding experiments.

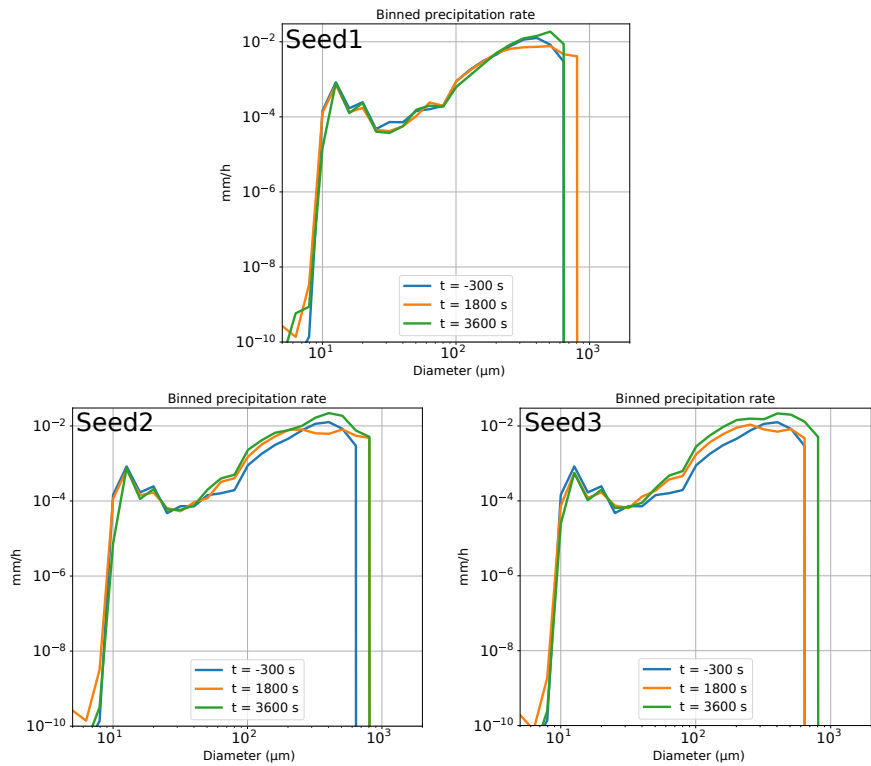


Figure 15. The contribution of hydrometeors to the total precipitation rate at cloud base as a function of size before (-300 s) and after (1800 s and 3600 s) the particle injection in the seeding experiments.